nation follows. On the basis of the information available, the triangle with sides **b**, **c** and **d** could just as well have been attached to the side **b** of the alternative dashed-line triangle. The magnitudes $|F_{\lambda \mathbf{h}}|$, $|F_{\lambda \bar{\mathbf{h}}}|$ and $|F^n_{2,\mathbf{h}}|$ would still be preserved as well as the assumed value for $\varphi^n_{2,\mathbf{h}}$. As seen in Fig. 1, such a triangle with sides of length **b**, **c** and **d** has been attached to the dashed triangle with the common base of vectors of length **c** and **d** extending far to the left. This determines an alternative and quite different vector, $F^n_{1,\mathbf{h}}$. It is quite long, about 2·4 times longer than the initially determined $|F^n_{1,\mathbf{h}}|$, extending as a dashed line from the origin to the base of the vectors of length **c** and **d**. The associated angle, $\varphi^n_{1,\mathbf{h}}$, is also rotated somewhat more than 90° farther than the initially determined $\varphi^n_{1,\mathbf{h}}$. The magnitude of the initial $|F^n_{1,\mathbf{h}}|$ is about 0·63 of the average value of $|F_{\lambda \mathbf{h}}|$ and $|F_{\lambda \bar{\mathbf{h}}}|$ and that of the alternative is about 1·5 times larger.

It is evident now from Fig. 1 how two alternative sets of results arise and that the alternatives would be distinguishable by use of approximate knowledge of the value of $|F^n_{1,\mathbf{h}}|$. It is of interest to review the assumptions inherent in the diagram as they relate to practical circumstances. There are experimental errors in $|F_{\lambda \mathbf{h}}|$ and $|F_{\lambda \bar{\mathbf{h}}}|$ and $|F^n_{2,\mathbf{h}}|$ can be obtained only approximately from the latter two intensities. The arbitrariness of $\varphi^n_{2,\mathbf{h}}$ does not play a role in the calculations since the quantity evaluated is $\varphi^n_{1,\mathbf{h}} - \varphi^n_{2,\mathbf{h}}$, which is invariant to rotation of the diagram in Fig. 1 around the origin. The effects of the various uncertainties are illustrated in the test calculations. Because of the uncertainties, the variation of starting values for $|F^n_{1,\mathbf{h}}|$ and, on occasion, $|F^n_{2,\mathbf{h}}|$ was introduced into the calculations in order to explore the field of convergence. With the computer used for the test calculations, 6000 distinct least-squares computations were performed in one minute.

The diagram in Fig. 1 emphasizes the important practical significance of having additional information concerning $|F^n_{1,\mathbf{h}}|$, $|F^n_{2,\mathbf{h}}|$ and $\varphi^n_{2,\mathbf{h}}$. As noted, information concerning $|F^n_{1,\mathbf{h}}|$ is available from an isomorphous replacement experiment since $|F^n_{1,\mathbf{h}}|$ represents the magnitude of the structure factor for the native substance. If the structure of the anomalous scatterers is determined initially, values for the $|F^n_{2,\mathbf{h}}|$ are available to enhance the accuracy of the calculations and values for the $\varphi^n_{2,\mathbf{h}}$ are available for the evaluation of the $\varphi^n_{1,\mathbf{h}}$ from values of the $\varphi^n_{1,\mathbf{h}} - \varphi^n_{2,\mathbf{h}}$. The immediate calculation of the electron distribution of the structure of interest would follow.

References

DALE, D., HODGKIN, D. C. & VENKATESAN, K. (1963). *Crystallography and Crystal Perfection*, edited by G. N. RAMACHANDRAN, pp. 237-242. New York, London: Academic Press.

GIACOVAZZO, C. (1983). *Acta Cryst.* A**39**, 585-592.

HAUPTMAN, H. (1982). *Acta Cryst.* A**38**, 632-641.

HENDRICKSON, W. A. & TEETER, M. (1981). *Nature (London)*, **290**, 107-113.

KARLE, J. (1980). *Int. J. Quantum Chem.* **7**, 357-367.

KARLE, J. (1984*a*). *Acta Cryst.* A**40**, 1-4.

KARLE, J. (1984*b*). *Acta Cryst.* A**40**, 4-11.

KARLE, J. (1984*c*). *Acta Cryst.* A**40**, 526-531.

PEERDEMAN, A. F. & BIJVOET, J. M. (1956). *Acta Cryst.* **9**, 1012-1015.

RAMACHANDRAN, G. N. & RAMAN, S. (1956). *Curr. Sci.* **25**, 348-351.

SHMUELI, U., WEISS, G. H., KIEFER, J. E. & WILSON, A. J. C. (1984). *Acta Cryst.* A**40**, 651-660.

TIMKOVICH, R. & DICKERSON, R. E. (1976). *J. Biol. Chem.* **251**, 4033-4046.

WOOLFSON, M. M. (1984). *Acta Cryst.* A**40**, 32-34.

Acta Cryst. (1985). A**41**, 394-399

A Comparison of Weissenberg and Diffractometer Methods for the Measurement of Diffuse Scattering from Disordered Molecular Crystals

BY T. R. WELBERRY

Research School of Chemistry, Australian National University, GPO Box 4, Canberra City, ACT 2601, *Australia*

AND A. M. GLAZER

*Clarendon Laboratory, Parks Road, Oxford OX*1 3*PU, England*

(*Received* 29 *May* 1984; *accepted* 28 *February* 1985)

Abstract

Diffuse X-ray scattering from a disordered molecular crystal [1,4-dibromo-2,5-diethyl-3,6-dimethylbenzene (BEMB1)] has been measured by diffractometer and conventional Weissenberg-film techniques, and a detailed comparison of the two sets of data has been made. An interexperimental agreement factor between the the two sets of intensities was about 22%. Statistical tests on the data revealed that a substantial part of this discrepancy was mainly due to systematic differences attributable to alignment problems associ-

0108-7673/85/040394-06$01.50

ated with the need to use large (>0·5 mm diameter) crystals. It is stressed that X-ray diffuse scattering can be easily and rapidly measured on a diffractometer as part of the normal process of structure determination.

Introduction

Substitutional or orientational disorder occurs widely throughout many branches of Crystallography. But while conventional structure solution and refinement using Bragg-reflection data has become more or less a routine operation, the measurement and interpretation of diffuse X-ray scattering for problems involving disorder is still performed on a largely *ad hoc* basis. Recently we have sought to develop methods, using conventional Weissenberg equipment, to make the systematic study of disorder problems in molecular crystals a more routine process (Epstein, Welberry & Jones, 1982; Welberry, Jones & Epstein, 1982; Epstein & Welberry, 1983). There have been few cases where a diffractometer has been used to measure whole reciprocal layer sections [see, for example, Singh & Glazer (1981) and Staknicka & Glazer (1984)]. The present study, in which diffuse scattering data have been collected on a diffractometer, was undertaken in order to compare, for the first time, diffractometer with the Weissenberg-film method in order to establish the accuracy, reliability and convenience of each method.

While there have been extensive comparisons between photographic and diffractometer methods for Bragg scattering, it is important to realise that for diffuse scattering the problems are rather different. With film techniques a large part of reciprocal space is surveyed on one film, whereas with the diffractometer, measurements are made at those points in reciprocal space predetermined by the operator. As film techniques have predominated in this field in the past we felt it useful to show that the diffractometer can also be used without very much difference in exposure time when working at a comparable resolution to the Weissenberg method.

Unlike the Bragg-reflection experiment in which intensities are measured relative to a local background, the origin of which is usually of no concern, for diffuse scattering, because of substitutional or orientational disorder, no simple 'background' measurement is available. Such unwanted additional scattering may be due to a variety of sources, such as fluorescence, air scattering, Compton scattering, thermal diffuse scattering (TDS), *etc.* In our analysis of the disorder diffuse scattering (hereafter referred to as DDS), account is taken of these other sources of scattering by using an empirical background correction for scattering, which is a function of the scattering angle, θ, alone (Welberry, 1983), and data-selection procedures which attempt to avoid localized regions of unwanted scattering. In order to be able to assess the validity of these procedures and to avoid any systematic errors they might introduce, it is important that the errors in the experimental data should be precisely known. For the diffractometer experiment the estimated errors obtained from counting statistics provide a useful source of such information, but for the film-based experiments errors are more difficult to quantify.

The material chosen for the present study was the compound 1,4-dibromo-2,5-diethyl-3,6-dimethylbenzene (BEMB1), $C_{12}H_{16}Br_2$ (Wood, Welberry & Puza, 1984), for which suitable spherical crystals were available. This compound which crystallizes in space group $P2_1$ with $a=9{\cdot}084$, $b=4{\cdot}459$, $c=17{\cdot}940$ Å, $\beta=122{\cdot}82°$, is one of a number of organic molecular crystals we are currently studying which exhibit static orientational disorder because of the similarity in size of the bromo and methyl substituents (see Fig. 1). A detailed study of this disorder is in progress. In the course of the study, diffractometer data were collected for six reciprocal lattice sections. In this paper we concentrate on the data obtained for the $(h0l)$ section, which we compare with previously obtained film data.

Film-data collection

Film data were obtained from conventional Weissenberg films (Agfa Osray M3, Kodak D19 developer) taken on a Stoe 28·65 mm radius Weissenberg camera, using graphite-monochromated Cu $K\alpha$ radiation. An approximately spherical crystal, 0·5 mm in diameter, was used, with a 0·8 mm diameter collimator. This was one of the standard Stoe-supplied collimators which protudes into the camera to within approximately 10 mm of the sample, thereby keeping air scattering to moderately low levels. The film was exposed for 3 days using a 1 mm layer-screen gap width and a 200° oscillation range with a film movement of 1 mm per 2°. The effect of the screen-width setting on the resolution of the diffuse scattering has been discussed in a previous paper (Welberry, 1983).

Intensity measurements were made from the film using an Optronics P-1700 Photomation system. Welberry & Jones (1980) have described the way in which this system may be used to scan the Weissenberg film and, after suitable background correction, contrast enhancement, and removal of the Weissenberg distortion, to write the intensity data back on to film to

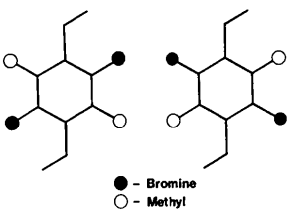

Fig. 1. The two orientations of the molecule of BEMB1 which give rise to the disorder.

give an undistorted picture of the diffuse scattering in reciprocal space. In Fig. 2(*a*) we show for later comparison such a photographic image of the (*h*0*l*) section for BEMB1.

For the purposes of fitting a calculated model of the DDS to the observed DDS by least squares (as described, for example, in Epstein & Welberry, 1983), intensity measurements are made at discrete points in reciprocal space. To achieve this, reciprocal coordinates on the film are defined precisely by performing a least-squares fit to the positions of a selected number of Bragg reflections, which are obtained from an initial scan of the film. In this process three reciprocal cell parameters, the camera radius R, and two film-origin position constants X_o and Y_o are refined. The resulting residual error in the calculated film coordinates for any reflection is typically about 0·1 mm.

Having defined positions on the film in terms of the constants R, X_o, Y_o, and the reciprocal cell constants a^*, β^*, and c^*, intensities are measured sequentially in a manner analogous to that on an automatic diffractometer. In the present study measurements for the (*h*0*l*) section were made on a grid $a^*/10$ by $c^*/5$ in the range $5<2\theta<51{\cdot}2°$, which corresponds to the range covered by the photographic image in Fig. 2(*a*). This was achieved with a range of $h=0$ to -5 and $l=-11$ to $+11$. In all, measurements were made at 3354 points.

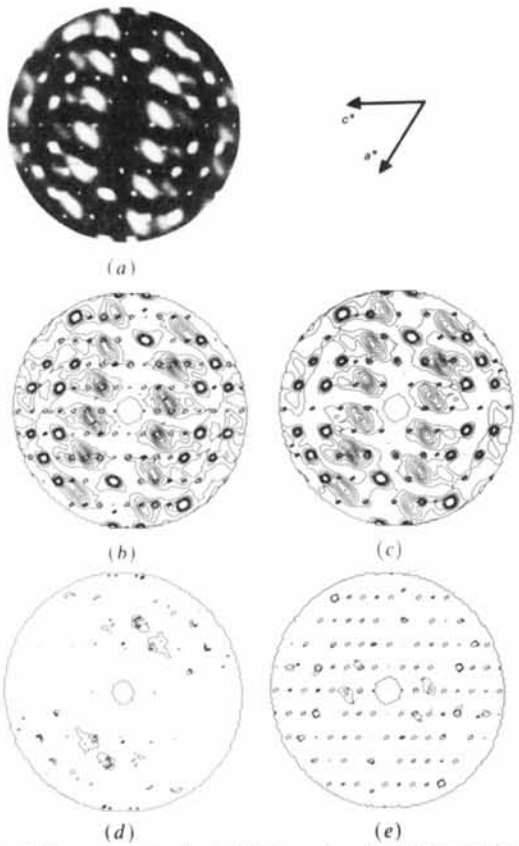

Fig. 2. Diffuse scattering in the (*h*0*l*) section of BEMB1. (*a*) Photographic image obtained by previous methods (see text). (*b*) Contour plot of the diffractometer data. Each contour represents 3·5 counts s^{-1}. (*c*) The film data on the same scale as (*b*). (*d*) Difference contours on the same scale as (*b*) and (*c*), for which the film intensities are greater than the diffractometer intensities. (*e*) Difference contours on the same scale as (*b*) and (*c*), for which the diffractometer intensities exceed the film intensities.

For each data point the value of the intensity was obtained as the average of nine optical density readings on a 3×3 array of pixels on the 100 μm raster grid of the Photomation scanner: *i.e.* from an area of the film 0·3×0·3 mm. An estimate of the standard deviation, σ_F, was obtained from the second moment of the nine readings about the mean. Previous experience in producing photographic images, such as that in Fig. 2(*a*), had tended to suggest that some benefit was obtained by using a larger Photomation scanning aperture (while maintaining the same raster grid), since this produces a less noisy photographic image without seeming to lose significant resolution. Two data sets were therefore taken from each film; the first using an aperture of 200 μm and the second one of 100 μm – the same as the raster increment.

Diffractometer-data collection

Diffractometer measurements were made on a Stoe (STADI-2) two-circle diffractometer at the Clarendon Laboratory, Oxford, using graphite-monochromated Cu $K\alpha$ radiation. The sample used for the (*h*0*l*) measurements was a spherical crystal of diameter 0·65 mm. This sample was chosen from among the small number of available crystals that had been ground to approximately spherical shape. The size was close to what was considered the maximum realistic value that could be used without encountering serious problems of non-uniform illumination. The diffractometer was set up with the detector 125 mm from the sample. A vertical detector-slit width of 4 mm was selected to give comparable resolution to the 1 mm layer-screen gap in the film equipment. The horizontal detector-slit width, which corresponds to resolution in θ and which has no counterpart on the Weissenberg camera, was set at 2 mm. Stationary counts of 100 s were made at points in one half of reciprocal space on a grid $a^*/10$ by $c^*/5$ in the range $5<2\theta<51{\cdot}2°$, resulting in the same 3354 data points as for the film data. The counting time was chosen after some initial tests to achieve counting errors in the intensity measurements of less than 10%. The total data collection for the section, including crystal alignment and substantial 'dead-time' between each measurement, was about 1 week, of which about 4 days was actual counting time.

To give an indication of the magnitude of the scattering signal which we are endeavouring to measure in this experiment, note the comparable magnitudes of the diffuse scattering and the Bragg-peak

intensities. Typical diffractometer counts in a strong diffuse peak (say at $h=1{\cdot}2$, $l=-3{\cdot}4$) were about $50\ s^{-1}$. In comparison, the strong Bragg peak 104 gave counts of $1{\cdot}4\times10^6\ s^{-1}$ and saturated the detector even with four attenuation filters in place.

Another aspect was revealed by some preliminary experiments in which Mo $K\alpha$ radiation was used. The mass absorption coefficients for bromine using Mo or Cu $K\alpha$ radiation are not too dissimilar ($\mu/\rho=7{\cdot}98$ and $9{\cdot}96\ mm^2\ kg^{-1}$ respectively), and a survey of the literature reveals that structures containing bromine have been determined using both radiations with almost equal frequency. The K absorption edge for bromine, however, occurs at 0·92 Å. This means that, although the absorption of the two radiations is similar in magnitude, the processes involved are very different. While the absorption of Mo $K\alpha$ will excite the bromine K fluorescence, the Cu $K\alpha$ will only excite the L and M fluorescence. The latter, being very soft radiations, will largely be attenuated before reaching the counter, while the former will be little affected over the same path length. Although fluorescence for Bragg-reflection analysis is not normally considered a severe problem when the excitation wavelength is as far from the absorption edge as Mo $K\alpha$ is from the Br K edge, the presence of even quite low levels of fluorescence may be quite intolerable for diffuse-scattering experiments such as described here. In the present experiment preliminary tests using Mo $K\alpha$ revealed that only about 10% of the diffuse intensity counts were due to the disorder, even for the strongest diffuse peaks.

Comparison of the Weissenberg and diffractometer data

(*a*) *Background correction and data selection*

Before a comparison of the two types of data was made, each was treated by our standard background-correction procedure. This procedure (see Welberry, 1983) makes the assumption that at any particular value of the diffraction angle θ there will be some point in the diffuse pattern where the DDS is zero. This assumption appears to be well justified in the present case of the ($h0l$) section of BEMB1, where calculation of the random diffuse pattern shows zero intensity along a line through the origin extending to the edge of the region covered, midway between the rows of strong diffuse maxima that run almost vertically in Fig. 2(*a*). For the treatment of both film and diffractometer data, data were partitioned into 0·25° ranges of θ and a background value was taken as the lowest intensity occurring in each θ range.

It was found that the background curves were different in the two experiments. This may be explained by the differences in the experimental conditions. First, the film background contains a constant component due to the fog-level of the film, so that the overall level is higher. The different variation with θ may be explained by the difference in the way the X-rays are detected in the two experiments. In the diffractometer experiment the horizontal detector slit excludes any scattering outside a narrow angular range centred on the crystal. For relatively high diffraction angles much of the air scattering, which occurs in the main beam before incidence on the crystal, will thus be excluded. For low diffraction angles this scattering arrives at the counter from approximately the same direction as the scattering from the crystal, and a larger proportion of it will be counted. For the film experiment, scattering from the whole region in which the direct beam passes through air, is incident on every part of the film.

Before being used to correct the intensity data, the background curves were smoothed using the scientific subroutine *SE*15 (IBM, 1968). Then the observed intensity, I_o, was taken as,

$$I_o = I_m - I_b$$

where I_m is the value actually measured and I_b is the appropriate background obtained from the smoothed curve. For both film and diffractometer data the estimated standard deviation, σ, of I_o was taken to be the same as that for I_m: *i.e.* the error in estimating the background was neglected. This is justified on the grounds that many measurements contribute to the estimation of the background at a particular point.

In addition to the DDS both sets of data include Bragg peaks and strong acoustic TDS, both of which required exclusion before a comparison could be made. Selection was performed by comparison of the data with a calculated model of the disorder. Observed data which were greater than the calculated value by more than 6σ were flagged for omission as being Bragg reflections or TDS. Of the original 3354 data approximately 500 were omitted. The film and diffractometer data were scaled together using only the unflagged data to determine the scale factor.

(*b*) *Contour plots*

Contour plots of the diffractometer and film data are shown in Fig. 2(*b*) and (*c*) respectively. Each contour corresponds to $3{\cdot}5\ s^{-1}$ counts in the diffractometer experiment. The highest contour shown corresponds to $31{\cdot}5\ s^{-1}$ counts and the strong TDS peaks, which have intensities far higher than this, are clearly distinguishable by their closely spaced contours and white centres. Superficially the two plots appear very similar and show close resemblance to the photographic image of Fig. 2(*a*).

Close agreement between the two sets of data is also demonstrated by difference plots which are shown in Figs. 2(*d*) and (*e*). Fig. 2(*d*) shows difference contours for which the diffractometer intensities

are greater. In both the contour interval is the same as in the plots of Figs. 2(*b*) and (*c*). Each of the difference plots shows a region where there is a significant difference between the two sets of diffuse-scattering data of about one contour level. In Fig. 2(*d*) this is in the top right (and bottom left) quadrants. Note that one of the two main peaks is associated with the strong TDS peak around the Bragg reflection $30\bar{2}$. A number of smaller (in area) peaks are all associated with other TDS peaks which were omitted from the scaling procedure. Fig. 2(*e*) shows a region near the Bragg reflection 003 and a smaller region near $\bar{1}03$ for which the diffractometer intensities are greater than the film intensities. Other significant regions on this plot are all associated with other TDS peaks. It is clear that Bragg peaks are invariably measured to be higher in the diffractometer experiment. This is because on the film these would be well beyond the film saturation exposure limit.

We attribute the sometimes quite marked differences in the strong TDS peaks which show up in these difference plots to the difference in spatial resolution inherent in the two experiments. Although the resolution limitation due to the Weissenberg geometry and layer-screen settings was chosen to be comparable in the two experiments, other aspects of the resolution are considerably better in the diffractometer experiment because of the greater crystal-to-detector distance. A typical Bragg-peak width in the diffractometer experiment was 0·5° (in ω–2θ) compared with about 2° for the film experiment. This 'smearing' of the pattern affects both Bragg and diffuse scattering alike. Its effect on the diffuse pattern in the film experiment is of a similar magnitude to that due to the layer-screen setting, and is not considered to be of great importance for the relatively short-range correlations in which we are interested. The only way that this aspect of the film experiment could be improved would be to increase the crystal-to-film distance or decrease the size of the crystal, with considerable loss of intensity in either case.

(*c*) *Normal probability plots*

In order to test further the agreement between the film and diffractometer sets of data and their corresponding standard deviations, we have used normal probability plot analyses, after the manner described by Abrahams & Keve (1971). We use the statistic,

$$\delta m_i = [I_F(i) - I_D(i)]/[\sigma_F^2(i) + \sigma_D^2(i)]^{1/2} \quad (1)$$

where $I_F(i)$ is the intensity at the ith data point in the film-data set, and $\sigma_F(i)$ its corresponding standard deviation. Equation (1) refers to data that are correctly put on the same scale. To construct the normal probability plot, the quantities δm_i are rearranged in order of increasing magnitude, *i.e.* as order statistics, and plotted against x_i, the values expected for a normal distribution. The distribution of δm_i is Gaussian if the $I_F(i)$, $I_D(i)$ contain only random errors and the $\sigma_F(i)$, $\sigma_D(i)$ are correct. If this ideal is met the resulting normal probability plot will be a straight line of slope 1·0 passing through the origin.

Figs. 3(*a*) and (*b*) show normal probability plots for the comparison of the diffractometer data with the 100 and 200 μm film data respectively. Both plots are reasonably close to straight lines, particularly over the important central region, but in each case the slope is considerably greater than 1·0; 1·35 for the 100 μm and 1·8 for the 200 μm data. These plots appear to indicate that the standard deviations are underestimated in both cases but otherwise reasonably follow a normal distribution. A plot in reciprocal space of those data points, for which $\delta m_i < 0{\cdot}0$, indicated a systematic distribution of errors, varying largely as a function of ω.

Conclusion

One result emerging from this study is that it has been established that the errors in our measurements of DDS intensities have a relatively large systematic component under the experimental conditions currently used. Although random errors in both film and diffractometer data were only of about 9%, the agreement between the two data sets was about 22%, and the distribution of the differences indicated a strong dependence on the crystal orientation, ω. Such variations with ω may be due to a number of causes, such as beam inhomogeneity coupled with imperfect crystal centring and alignment, or imperfectly spherical crystal shape and high absorption. Even with the most careful experimental procedures these problems are difficult to avoid completely when large crystals must be used. The study has clearly indicated the need for full use to be made of available symmetry to check on the internal consistency of data from a given sample. This can currently be done for film data with very little extra work since symmetry-related data may be obtained from the two halves of a stan-

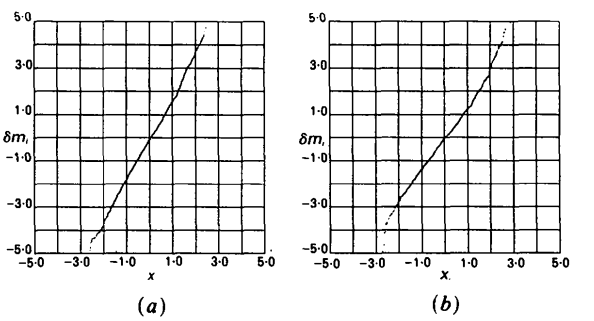

Fig. 3. Normal probability plots for (*a*) the 100 μm film data and (*b*) the 200 μm film data, compared with the diffractometer data.

dard Weissenberg film, but for diffractometer data further counting would be required.

Although the estimated standard deviations for the film data obtained from the densitometer measurements are a useful guide in assessing the level of the random errors in the data, neither the 100 μm nor the 200 μm data-collection method gave a true measure of the errors. We conclude, therefore, that great emphasis should not be placed on these values in devising a weighting scheme to be used in the least-squares analysis of the data.

As a result of this work we have demonstrated that the diffractometer can be used for obtaining high-quality diffuse-scattering measurements in about the same time as the Weissenberg method (and quicker than using oscillation techniques as these require many separate exposures and unravelling of the diffraction patterns) and with about the same or better resolution. Normally the diffractometer is used by structural cyrstallographers for collecting only Bragg reflections and this must mean that a great deal of useful and informative diffuse scattering is missed. We hope that the present work will stimulate others to use their diffractometers at least to *look* for diffuse scattering as a routine part of their structural study. In some cases this may provide important clues to the solution of the structure, particularly when normal refinement methods have failed.

We are grateful to J. Siripitayananon for recording the film data, and K. Owen, J. Moxon and F. Wondre for technical assistance. One of us (TRW) is grateful to the Science and Engineering Research Council for a Senior Visiting Fellowship during the tenure of which much of this work was carried out.

References

ABRAHAMS, S. C. & KEVE, E. T. (1971). *Acta Cryst.* A**27**, 157–165.

EPSTEIN, J. & WELBERRY, T. R. (1983). *Acta Cryst.* A**39**, 882–892.

EPSTEIN, J., WELBERRY, T. R. & JONES, R. D. G. (1982). *Acta Cryst.* A**38**, 611–618.

IBM (1968). *System/360 Scientific Subroutine Package* (360A-CM-03X). New York: IBM Technical Publication Dept.

SINGH, S. & GLAZER, A. M. (1981). *Acta Cryst.* A**37**, 804–808.

STADNICKA, K. & GLAZER, A. M. (1984). *Acta Cryst.* B**40**, 139–145.

WELBERRY, T. R. (1983). *J. Appl. Cryst.* **16**, 192–197.

WELBERRY, T. R. & JONES, R. D. G. (1980). *J. Appl. Cryst.* **13**, 244–251.

WELBERRY, T. R., JONES, R. D. G. & EPSTEIN, J. (1982). *Acta Cryst.* B**38**, 1518–1525.

WOOD, R. A., WELBERRY, T. R. & PUZA, M. (1984). *Acta Cryst.* C**40**, 1255–1260.

SHORT COMMUNICATION

Contributions intended for publication under this heading should be expressly so marked; they should not exceed about 1000 *words; they should be forwarded in the usual way to the appropriate Co-editor; they will be published as speedily as possible.*

Acta Cryst. (1985). A**41**, 399

Standard crystallographic file structure – 84. By I. D. BROWN (SCFS Project Coordinator), *Institute for Materials Research, McMaster University, Hamilton, Ontario, Canada L8S 4M1*

(*Received* 17 *January* 1985; *accepted* 19 *February* 1985)

Abstract

The Commissions on Crystallographic Data and on Crystallographic Computing of the International Union of Crystallography have approved a revised version (SCFS-84) of the Standard Crystallographic File Structure reported in *Acta Cryst.* (1983), A**39**, 216–224. The major change involves the definition of new sections describing the space group (SG NAME) and atomic coordinates (ATOMS) to supersede those in the earlier standard (SPACE GROUP and ATOM respectively). A new section (BONDS) is defined and other sections are extended to include a wider range of data. Copies of SCFS-84 may be obtained from the author or the Executive Secretary of the International Union of Crystallography.

The standard described in the *Abstract* has been deposited with the British Library Lending Division as Supplementary Publication No. SUP 42068 (33 pp.). Copies may be obtained through The Executive Secretary, International Union of Crystallography, 5 Abbey Square, Chester CH1 2HU, England. Copies may also be obtained from the author.

0108-7673/85/040399-01$01.50